

Accepted Manuscript

Carbonate ions, orbits and Mg/Ca at ODP 1123

Simon J. Crowhurst, Heiko Pälike, Ros E.M. Rickaby

PII: S0016-7037(18)30164-9

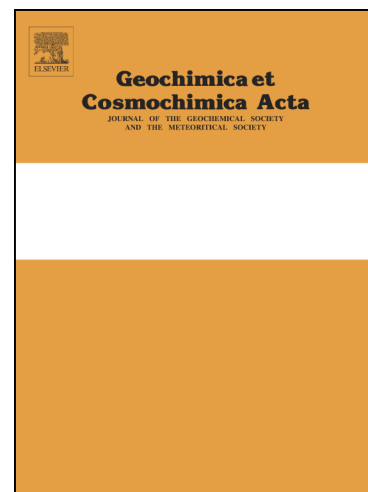
DOI: <https://doi.org/10.1016/j.gca.2018.03.013>

Reference: GCA 10707

To appear in: *Geochimica et Cosmochimica Acta*

Received Date: 31 July 2017

Accepted Date: 8 March 2018



Please cite this article as: Crowhurst, S.J., Pälike, H., Rickaby, R.E.M., Carbonate ions, orbits and Mg/Ca at ODP 1123, *Geochimica et Cosmochimica Acta* (2018), doi: <https://doi.org/10.1016/j.gca.2018.03.013>

This is a PDF file of an unedited manuscript that has been accepted for publication. As a service to our customers we are providing this early version of the manuscript. The manuscript will undergo copyediting, typesetting, and review of the resulting proof before it is published in its final form. Please note that during the production process errors may be discovered which could affect the content, and all legal disclaimers that apply to the journal pertain.

Carbonate ions, orbits and Mg/Ca at ODP 1123Simon J Crowhurst^a, Heiko Pälike^b Ros E. M. Rickaby^c^aDepartment of Earth Sciences, University of Cambridge, Downing Street, Cambridge, CB3 3EQ, United Kingdom, ^b MARUM Center for Marine Environmental Sciences, University of Bremen, 28359 Bremen, Germany ^cDepartment of Earth Sciences, University of Oxford, South Parks Road, Oxford, OX1 3AN, United KingdomEmail: sjc13@cam.ac.uk (corresponding author, Department of Earth Sciences, Downing Street, Cambridge CB2 2EQ, UK)**Abstract**

The accuracy of the magnesium/calcium palaeotemperature proxy has been questioned, in particular because the ratio of magnesium to calcium in foraminiferal tests could be affected by local or global changes in carbonate ion concentrations in deep water. A related question regarding the technique is its problematic phase relationship to orbital eccentricity: Mg/Ca records of intermediate and deep waters typically show a phase lead with respect to orbital eccentricity. This calls into question either the validity of the Mg/Ca palaeotemperature proxy, or the assumption that orbital eccentricity is pacing the 100 kyr climate oscillations, or both. This paper addresses these questions, and suggests that a phase lead of the type observed at ODP 1123 is unlikely to be generated by the operation of the carbonate ion effect, and might be attributable to heat storage in the oceans during low eccentricity episodes.

1. Introduction

Mg/Ca palaeothermometry is a technique used to separate out the temperature and ice volume components of the marine oxygen isotope records obtained from foraminiferal calcite (Lear et al. 2000, Elderfield et al., 2012). Shackleton (2000) used a spectral analytical technique to achieve the same separation with closely comparable results; a very significant portion – perhaps 50% -of the marine isotopic foraminiferal $\delta^{18}\text{O}$ record, even in the relatively stable deep ocean, is attributable to temperature changes rather than to global ice volume /sea level changes.

A complication is that Mg/Ca ratios are potentially affected by changes in the carbonate saturation of the deep ocean – the so-called saturation state effect (Yu and Broecker 2010, responded to by Sosdian and Rosenthal 2010) . Harry Elderfield addressed this misgiving in part by using the infaunal benthic genus *Uvigerina* rather than the deep dwelling, but epifaunal, *Cibicidoides wuellerstorfi* , since *wuellerstorfi* would have been more exposed to immediate changes in deep and intermediate water

carbonate concentration, which could have offset its Mg/Ca ratios (Elderfield, 1996). Elderfield et al. 2010 and 2012 used infaunal foraminifera to attempt to avoid such effects on the Mg/Ca ratios. The effectiveness of different species as proxies for different water properties was investigated by Elmore et al. 2015, who found that Mg/Ca ratios in *U. peregrina* were the most effective proxy for water palaeotemperatures at intermediate water depths while B/Ca ratios in *P. wuellerstorfi* were the most effective proxy for carbonate ion concentrations.

A related question is the confidence that can be placed in the Mg/Ca based palaeotemperature reconstructions, given the puzzling relationship between the temperatures indicated by the Mg/Ca proxy and the supposed forcing or pacing of climate by orbital eccentricity. A consistent observation of Mg/Ca studies is that the warmings of intermediate and deep water precede the upturn in the eccentricity curve normally used as the indicator for the eccentricity-related warming of Earth's climate. (Sosdian and Rosenthal, 2010; Elderfield et al. 2010; Elderfield et al. 2012). This paper addresses the specific misgiving about the Mg/Ca proxy, that its phase relationship to orbital eccentricity is problematic.

Earth's orbital variations, and the planet's climatological behaviour, appear to have been closely linked throughout the Phanerozoic. The waxing and waning of gigantic ice sheets has dominated the climatic history of the last million years, and interpretations of the orbital forcing involved have helped to create detailed and widely applicable timescales for the interval (eg Lisiecki and Raymo, 2005, Gradstein, 2012). Since the ground-breaking study of marine isotopic and faunal count sequences by Hays et al. (1976) it has been clear that the main periodicities of climate change on multi-millennial timescales coincide with the periodicities of the principle changes in the Earth's orbital geometry - precession, obliquity, and eccentricity.

Changes in the ellipticity of Earth's orbit, caused by gravitational interactions with other planets, have periodicities of around 100 and 400 kyr, as well as much longer-term cycles on million year timescales (Liebrand et al. 2016). Obliquity (changes in the amount of tilt of the polar axis in relation to the orbital plane) currently operates with a periodicity of 41 kyr, and also has longer modulations at 176 kyr and 1.2 Myr. Precessional changes, which rotate the direction that the polar axes point towards in relation to the orbital plane, govern the intensity of the Earth's seasonality at different latitudes with periodicities of currently around 21 kyr, and are modulated in amplitude by the eccentricity cycle. Precessional

effects warm and cool the Northern and Southern hemispheres in antiphase (Raymo et al. 2006, Lisiecki 2010); when northern summers are warmest, those in the south are coolest.

While the effects of precession and obliquity can be understood as approximately linear responses to the calculated orbital forcing changes associated with them (Huybers 2006), climate forcing or pacing at eccentricity periods has proved harder to explain, and the effort to do so has generated a large number of explanatory models. These can be grouped into three broad categories, with some models overlapping several categories. Model group one, envisages nonlinear enhancement of eccentricity effects through the climate system (Imbrie et al. 1993). Model group two attributes the cyclicity to other aspects of orbital variation, such as orbital inclination or skipped obliquity cycles (Huybers 2007). Model group three largely attributes the extent of change, and in some models its timing, to stochastic processes (Ditlevsen 2009).

Hays, Imbrie and Shackleton (1976) referred not to climate forcing by eccentricity, but “pacing”, explicitly leaving the causative mechanisms open, because they were aware that there was a mismatch between the energy differences associated with the orbital variations at the eccentricity periodicities and the dramatic scale of 100,000 year climate oscillations. They commented: “specifically, we abandon the assumption of linearity” (p.1130), and favoured explanations in terms of differential rates of ice accumulation and loss. Shackleton (2000) argued that carbon dioxide could act as an amplifier of deglacial processes at the 100 kyr periodicity. Recent global climate models (Abe-Ouchi et al. 2013; Ganopolski et al. 2016) have indicated that a climate response at the 100,000 year periodicity can be driven by the climatic consequences of known insolation changes. These modelling observations were explained by a combination of the isostatic behaviour of ice sheets and the background levels of CO₂ during the Late Pleistocene. Huybers and Denton (2008) and Stott et al. (2007) investigated the relationship between insolation duration and insolation intensity for the shorter term precession cycle; here we consider the relationship of these two components to the eccentricity cycle.

The orbitally modulated incoming radiation (insolation) changes associated with the 100 kyr eccentricity cycle are often said to be too weak to explain the climate response at that periodicity. The net insolation change associated with the Earth's enhanced proximity to the sun at perihelion during periods of high eccentricity is relatively tiny; Ruddiman (2006) in a major review article, commented on the 100 kyr climatic cycles: “These responses cannot be explained by the very small insolation changes at the period

of orbital eccentricity, which amount to 1–2% of those at the periods of tilt and precession” (p3098). Lisiecki (2010, p349) commented that the “defining aspect of the 100,000-yr (100-kyr) problem is ... the lack of significant external forcing at that frequency”. Fig. 1 A and B show that insolation remains at closely equivalent levels through the 100,000 year cycle. It is blurred into dispersed “blobs” of geographically widely distributed insolation or broken up into angled “bars” which are antiphased between the poles, by the strengthening or weakening of precessional effects, which are modulated by eccentricity. Fig. 2 illustrates the discrepancy between the relative amplitudes of the forcing and response at eccentricity periodicities; while the climatic response at obliquity and precessional periodicities is reasonably proportional to the variance in the forcing – shown here as insolation at 65 degrees North – the 100 kyr climate cyclicity is disproportionate to the relatively tiny forcing at this periodicity.

Insolation forcing at eccentricity periodicities can be considered in terms of two powerful components, which arrive in antiphase: the insolation intensity changes associated with the reduction in distance to the sun at perihelion at times of high eccentricity, and the effects of seasonal extension of the warm season, caused by the operation of Kepler's second law, which states that a planet sweeps out equal area segments during equal time intervals in the course of its orbit. Because of this effect, a planet in an eccentric orbit travels along its orbit faster at perihelion and more slowly at aphelion relative to a stationary observer (Fig. 3). The two components of an eccentric orbit – insolation intensity and seasonal duration - almost exactly cancel each other out in terms of the energy received at the surface of the Earth's atmosphere over the course of the 100,000 year cycle, so that eccentricity is calculated to be a (net) weak forcing, with its principle climatic impact being through the amplitude modulation of the precessional cycles.

Today, the Earth's elliptical orbit around the Sun has a mean eccentricity of 0.0167. However this aspect of the orbital geometry varies with an approximately 100 kyr periodicity. 115,000 years ago it was 0.0439 and 216,000 years ago its value was close to 0.05 (Laskar et al. 2004).

Laskar et al. (2011) discussed the fact that while the annual mean temperature varies as function of e^2 , and is thus very small, the seasonal difference between perihelion and aphelion for Earth's surface temperature is approximated by the change of eccentricity times the absolute temperature, hence a change of eccentricity by 0.02 corresponds to a temperature change of about $0.02 \cdot 300\text{K} = 6\text{K}$.

This is more than enough temperature difference to drive the climatic change between glacial and interglacial states on a purely linear basis. However, the extension of seasonality is almost precisely balanced by the increase in the intensity of insolation caused by increased proximity to the sun during perihelion, and its reduction at aphelion, as described below.

The phase relationship between the eccentricity calculations and the geological record of climate change indicates that deglaciations and subsequent interglacials – relatively warm intervals of relatively low ice volume – are more closely associated with intervals of high eccentricity than with the intervals of extended seasonal warmth linked to low eccentricity (eg Hays et al, 1976, Kawamura et al., 2007). The extra insolation received as a result of increased proximity to the sun at perihelion during intervals of high eccentricity is neatly (though not completely) counterbalanced by a shortening of the period spent at perihelion. This is because of the effects described by Kepler's second law: a line segment joining a planet and the star that it orbits sweeps out equal areas during equal intervals of time, so that when the distance to the star is shorter, the planet travels faster in order to sweep out the same area, and comply with its Keplerian area-sweeping quota.

In this way, orbital configurations of high eccentricity, which make summer unusually warm in one hemisphere, also shorten it, since the Earth accelerates as it approaches perihelion and decelerates as it approaches aphelion. By the same token, when eccentricity is low and the orbit almost circular, the time spent in summer in the two hemispheres is extended, and the seasonal contrast in insolation is reduced; the summer is not particularly warm, but neither is the winter particularly cold.

At high eccentricity states, wintertime is prolonged and more severe in the hemisphere which is in summer at perihelion, when insolation is more intense. Conversely, a relatively low-temperature summertime is extended in the hemisphere which is in summer at aphelion. So the benefits of higher insolation at perihelion are counterbalanced by the extension of winter and the abbreviation of summer, leading to a negligible difference in insolation at the 100 kyr periodicity, at a particular latitude and for a particular date over the 100 kyr cycle. The energy differences associated with the eccentricity cycle are instead expressed in insolation intensity changes caused by being in summer at perihelion at high eccentricity states; in other words, the precessional climate cycle and the amplitude modulation of precession by eccentricity. In a similar way, the effects of higher insolation intensity at high eccentricity states are counterbalanced by extended, more evenly distributed insolation between the hemispheres

at low eccentricity states.

This counterbalancing of insolation makes the dual effect of eccentricity an apparently feeble driver of climate on a simple, black-body, radiation-experiencing sphere. A uniformly strong energy supply, delivered with varying hemispheric emphases caused by precession, is supplied to the planet at the 100 kyr periodicity (Fig. 1).

2. Methods and results

Two potential explanations for the Mg/Ca phase lead at eccentricity periodicities were investigated using time series analysis. The first was the possibility that the Mg/Ca record has been affected by carbonate ion concentration changes in the deep sea closely related to atmospheric CO₂ changes. The second hypothesis explored was the possibility that eccentricity affects the Earth's climate system by combining the effects of "normal" eccentricity (insolation intensity changes associated with higher eccentricity states) with the effects of "inverse" eccentricity: insolation duration changes associated with low eccentricity states, which we hypothesise to have a strongly lagged cumulative effect on the climate system.

The relationship between between the benthic foraminiferal calcite $\delta^{18}\text{O}$ and Mg/Ca records of ODP 1123 (Elderfield et al. 2012), and between the benthic calcite $\delta^{18}\text{O}$ and the deconvolved seawater $\delta^{18}\text{O}$ sequence – which approximately corresponds to ice volume and sea level – is shown in Fig. 4 panels A and B, on the LR04-based timescale of Elderfield et al. 2012. Fig. 5 shows the Mg/Ca record on that timescale after filtering the 100-kyr centred periodicities against a 100-kyr filter of the conventionally recognised orbital components at that periodicity (ETP, normalised eccentricity, "tilt" and precession). This illustrates the strong phase lead of the Mg/Ca (deep temperature) record relative to orbital eccentricity.

The phase relationship between orbital eccentricity (Laskar, 1990) and the Epica Dome C (EDC) timescale EDC3 (Jouzel et al., 2007) shows a very slight (2.7kyr) lead of the CO₂ record to orbital eccentricity, with a 90% confidence interval spanning about 2.5 kyr on either side of this estimate (Fig. 6). The phase offset of CO₂ relative to conventional eccentricity is therefore close to zero (0.2 kyr) at its lower 90% confidence boundary, as observed by Hodell et al. (2017). The Mg/Ca record, in contrast, shows the well-established (Sosdian and Rosenthal, 2010; Elderfield et al. 2010; Elderfield et al. 2012) phase lead

relative to eccentricity of around 10kyr on the EDC3 based timescale, effectively the same as its phase lead on the LR04 timescale. This re-emphasises that the pronounced phase lead of Mg/Ca to orbital eccentricity is not an artifact of a particular age model. The 90% confidence limit is equivalent to ± 3 kyr, so that the phase offset on this timescale is between about 7 and 13 kyr. There is therefore a significant lead of the Mg/Ca curve relative to atmospheric CO₂ as well as to orbital eccentricity.

The climate proxy record of ODP 1123 was re-tuned to match the chronology of the Antarctic CO₂ record using the ODP 1123 sea surface temperature data of Crundwell et al. 2008, assuming sea surface temperature changes at that site were essentially synchronous with Antarctic temperature changes recorded in the EDC3 deuterium record. This provides a chronological basis for comparing ODP 1123 and EDC3 climate proxies and their relationships to eccentricity (Fig. 7A).

The inverse relationship of carbonate ion effects to atmospheric CO₂ was indicated by Kerr et al. 2017. To investigate the range of possible relationships of CO₂-induced carbonate ion changes to climate oscillations, the Antarctic CO₂ signal (Lüthi et al. 2008), was inverted by multiplying the CO₂ values by minus one. The amplitude and phase offsets of the carbonate ion proxy required to effect the possible carbonate ion impacts on the climate/temperature record (eg the Mg/Ca sequence) were then explored using the spectral properties and phase consequences of varying amplitudes and phase offsets of the resultant “composite CO₂” record, which combines the normal-phase with the adjusted phase and amplitude, inverse CO₂ record (Fig. 7B).

This experiment was intended to explore the scale and nature of the overprint of the carbonate ion effect needed to produce a significant phase offset in a climate record, especially in relation to the probable source of global carbonate ion concentration changes at these periodicities – namely, atmospheric CO₂ changes. In this way, the CO₂ record is being used to evaluate the distortion that a carbonate ion effect might impose on a pure temperature record, such as Mg/Ca might provide if there were no carbonate ion distortion.

Adding a 10kyr lagged, half-amplitude inverse CO₂ (carbonate ion concentration) record to the CO₂ record produced a composite record with a 9 kyr phase lead with respect to orbital eccentricity, about the order of size of the observed Mg/Ca phase lead to eccentricity at ODP 1123 (Fig. 7B). A lagged inverse CO₂ effect of equivalent amplitude to the principle CO₂ effect - ie with a lagged inverse

component of equal amplitude to the amplitude of the standard CO₂ sequence - could generate a similar phase lead with a smaller lag of the inverse signal. However, the proxy Mg/Ca record produced by such a combination, assuming that the corresponding Mg/Ca sequence would behave similarly to the modified CO₂ sequence, is more “spiky”, with very short-lived interglacials, and so fails to match the Mg/Ca record in terms of morphology.

An alternative explanation of the phase lead of the Mg/Ca curve is combined eccentricity, which combines normal phase (standard eccentricity, effectively seasonal insolation intensity) with lagged inverse phase (low eccentricity, effectively seasonal insolation duration) sequences. The combined eccentricity series is constructed by multiplying the standard eccentricity curve by -1, lagging the product by 26 kyr, and adding it to the original eccentricity curve. Equal proportions of normal and lagged inverse eccentricity were used. This amplitude and lag of the combined curve were derived from the residuals obtained by subtracting normalised eccentricity from the 1123 Mg/Ca curve as described in Elderfield et al. (2012) supplementary material, and shown in Fig. 8.

To explore the potential explanatory power of “combined eccentricity” (normal plus lagged inverse eccentricity) we matched the amplitude of variation of the principle orbital periodicities (combined eccentricity, obliquity and precessional cyclicities) to match the mean amplitudes of variation of the equivalent periodicities in the benthic $\delta^{18}\text{O}$ sequence from ODP 1123 on its original LR04-based timescale (Elderfield et al. 2012) (Fig. 9).

The spectral and phase properties of this new amplitude-adjusted forcing/pacing model were then investigated. The spectral peak at 100 kyrs is well matched to that of the $\delta^{18}\text{O}$ sequence, which was primarily tuned to obliquity and precessional components (Lisiecki and Raymo 2005), and the phase at 100 kyr also closely matches that of the $\delta^{18}\text{O}$ record from ODP 1123 (Fig. 10). The Analyseries software package (Paillard et al. 1996) was used for all of these analyses.

Discussion

3.1 The phase lead at eccentricity periodicities, and carbonate ion variations

One possible explanation for the phase lead of Mg/Ca to eccentricity is that it might arise from carbonate ion [CO₃²⁻] saturation effects in the deep water close to the sediment surface, or by pore-water chemistry effects arising from interactions between the pore waters in the shallowest few

centimeters of sediment and the deep oceanic waters immediately above the sediment surface. Elderfield et al. (2010,2012) chose to measure Mg/Ca on infaunal species (*Uvigerina* spp.) rather than epibenthic species, in order to reduce the impact of deep water chemistry on the composition of the foraminiferal tests, assuming porewaters attain carbonate saturation within a few cm of the sediment/water interface. Carbonate ion concentrations are inversely related to atmospheric CO₂ (Kerr et al. 2017), and are therefore relatively high during glacials, which are associated with lower atmospheric CO₂ levels. Dissolution is therefore less likely during glacials than interglacials, in terms of the pH effects of lowered atmospheric CO₂ and increased carbonate ion, although the global effects of carbonate ion changes appear to be relatively small (Zeebe and Marchitto, 2010).

To evaluate the possibility that lower atmospheric CO₂ had induced an apparent early-phase warming in the Mg/Ca proxy record, we synchronised the 1123 Mg/Ca record with the Epica Dome C (EDC3) CO₂ record (Lüthi et al. 2008) as described above, not for the purposes of timescale improvement, but to address this question of the relative timing between the possible oceanic carbonate ion effects and the Antarctic CO₂ and ODP 1123 temperature records. If the Mg/Ca phase anomaly was caused by lower atmospheric CO₂ levels inducing higher carbonate ion concentrations and lower carbonate ion concentrations (undersaturation) associated with higher atmospheric CO₂, then the effects should be in antiphase with, or lag the antiphased record, of atmospheric CO₂.

The broad pattern (sense) of the Mg/Ca record, as would be expected for a record that is primarily recording ocean temperature, is essentially in-phase with the glacial-interglacial temperature oscillations recorded in the ice core deuterium record – ie it has the same direction, with higher values of Mg/Ca being associated with warmer temperatures. The Mg/Ca record is therefore also broadly in-phase with atmospheric CO₂, which matches Antarctic temperature closely; higher atmospheric CO₂ is in general associated with higher temperatures and lower ice volumes. A carbonate ion effect of inverse relationship to the CO₂ record (Kerr et al. 2017) would need to have an offset phase relationship to the EDC3 CO₂ record to have an effect other than a simple reduction of the amplitude of the Mg/Ca signal. We therefore investigated the effect of combining a lagged inverse component to the main CO₂ record to attempt to mimic the overprint of a carbonate ion effect on the overall Mg/Ca record.

We found that, as described above, a carbonate ion effect of significant amplitude and significantly lagged phase might be able to generate the sorts of phase relationship between Mg/Ca and eccentricity seen at ODP 1123, provided that a) raised carbonate ion concentrations produce raised Mg/Ca ratios and b) the effects of carbonate ion concentrations are significantly lagged relative to the original inverted CO₂ and c) that the carbonate ion and dissolution effects are large enough and of the right sign to overprint the Mg/Ca record in the direction required. It is however, debatable whether a carbonate ion effect of such a magnitude could have been produced by the glacial-interglacial carbonate ion changes, plus temperature effects, of the deep ocean, as far as these changes are currently understood. Note that a downcore dissolution impact of the carbonate ion effect simulated here would counteract the lag, because it would stratigraphically mimic a lead of the concentration change, making an even longer lag necessary. The accumulation rates at ODP 1123 imply that over 40cm of sediment would protect the original signal from geochemical changes occurring 10 kyr later, since pore waters appear to achieve saturation within a few cm of the sediment-water interface (Jahnke and Jahnke 2004).

Current estimates put the whole ocean change in carbonate ion concentration at +7 µmol/kg during the glacial cycle (Kerr et al., 2017). Using the sensitivity of Mg/Ca to change in carbonate ion of 0.0086 mmol/mol/µmol/kg for epifaunal species as an upper estimate of what infaunal species could experience (Elderfield et al. 2006), even a superimposed regional change of 30 µmol/kg in carbonate ion would induce a signal of only 0.258 mmol/mol in Mg/Ca. Stratification, carbon sequestration and circulation could all have regional effects, and change local carbonate ion quickly, but we can assume that on a global scale carbonate compensation will react with some temporal lag of dissolution, so overall deep ocean carbonate ion is a phase lagged inverse of pCO₂. It is therefore unlikely that the carbonate ion effect could be of sufficient amplitude (around half the size of the temperature effect) or of appropriate phase to generate the kind of phase offset seen – apparently globally - in the benthic Mg/Ca record. A phase offset for the carbonate saturation effect of greater than 10 kyr would require that modern pore waters should contain the carbonate ion saturation of the last glacial.

3.2 The operation of eccentricity cycles on the climate system

Harry Elderfield's separation of the temperature and ice volume components of the Southern Ocean benthic oxygen isotope record (Elderfield et al. 2010, Elderfield et al. 2012) suggested a novel way of thinking about some of the possible oceanographic processes generating its timing, involving differential responses to the components of orbital eccentricity.

If different "heat reservoirs" in the Earth's climate system - for example the oceans and the ice sheets - behave with different heat storage, movement and lag characteristics to the two components of the eccentricity cycle, the substantial energy budget associated with the eccentricity cyclicity as a whole could be translated into a very significant climatic impact, such as that observed over most of the last million years. If the observed phase lead of Mg/Ca to orbital eccentricity is not an artifact of carbonate ion concentration changes, then another possibility is that during glacials, the stratified ocean stores not just carbon dioxide - some of which it releases at deglaciations - but also heat .

The Earth's response to insolation through its complex climate system is far from simple. Vast ice sheets accumulate over much of the Northern hemisphere, taking tens of millennia to build, before melting away relatively rapidly to leave much smaller ice masses such as those existing today, in the present interglacial (the Holocene). While the huge northern and southern ice sheets exist, they affect the Earth's albedo, and its intricate oceanic circulation. The Earth's oceans store and redistribute heat around the planet in swirling, eddy-spawning currents that can take thousands of years to complete a cycle of exposure to the atmosphere.

During full glacial episodes, there is evidence that the oceans become relatively stratified and are potentially covered by a larger area of sea ice (Crosta et al. 1998, Stephens and Keeling, 2000), greatly reducing their exposure to the atmosphere, and preventing thermal and chemical equilibration with the atmosphere by some water masses. The oceans also appear capable of effectively sequestering large quantities of carbon dioxide from the atmosphere and other sources before releasing it periodically, around the time of deglaciations, as indicated by the Antarctic CO₂ records (Jaccard et al. 2016; Howe et al. 2016; Freeman et al. 2016).

3.3 Climatological phase leads with respect to insolation intensity at eccentricity periods

A puzzling aspect of the behaviour of several climate parameters - particularly those associated with carbon cycling, is that they appear to behave in 100 kyr cycles with phase leads - equivalent to several thousand years - with respect to conventionally expressed eccentricity forcing (ie net insolation intensity). This presents a causality problem: why should a parameter systematically change ahead of the factor that is supposed to be forcing or pacing it?

Ruddiman (2003) documented a range of such responses and highlighted the possibility of phase

distortion by rectification (truncation) of the sawtoothed eccentricity record, and the time series implication of such distortion. However, there is little evidence that the sedimentary record is often systematically distorted in this way. The full amplitude modulation of more rapid periodicities, precession in particular, would not survive such distortion, and yet is routinely observed (Hilgen 1991a;1991b; Hodell et al. 2013). Precessional and sub-Milankovitch oscillations are well and consistently preserved in many sedimentary environments including ice cores, marine, and lake cores such as Lake Baikal, and yet the amplitude modulation by eccentricity appears consistent (eg Lisiecki and Raymo 2005). So sedimentary distortion of the record seems to be an unlikely candidate for generating the observed lead.

In addition, an artifact of spectral analysis (which tends to detect periodicities in terms of their representation as sinusoids) would not explain the well documented early phasing of abrupt deglaciations when deglaciations are treated in isolation, as observed for example at Termination II (Thomas et al. 2009).

The problem becomes particularly acute when considering the deconvolution of the temperature and ice-volume components of the deep marine isotopic record. Using a spectral analytical comparison of ice core and oceanic records, Shackleton (2000) demonstrated that the phase of temperature change in the oceans leads the ice volume component of the deconvolved marine benthic $\delta^{18}\text{O}$ signal by around 10 kyr at eccentricity periodicities. A similar phase lead was also identified by Sosdian and Rosenthal (2009) from a Mg/Ca palaeotemperature record from a North Atlantic DSDP Site 607. This observation was substantiated and more clearly resolved by Elderfield et al. (2012) who ran paired $\delta^{18}\text{O}$ and Mg/Ca samples of infaunal benthic foraminifera from core ODP 1123 from the Chatham Rise in the Pacific Ocean (Fig. 4). They showed that the temperature component of the $\delta^{18}\text{O}$ record leads the ice volume component by some 11,000 years at eccentricity periodicities, which puts the temperature component of the benthic $\delta^{18}\text{O}$ signal well ahead of its supposed forcing by insolation intensity changes caused by eccentricity. This phase lead can be seen in the 100kyr filtered record comparison of orbital forcing (expressed as normalised ETP) and the ODP 1123 Mg/Ca (deep water temperature) record (Fig. 5). For the last 800 kyr on the LR04 timescale, the phase lead of ODP 1123 Mg/Ca relative to ETP is 10.5 kyr, with a 95% confidence interval of 6.4 kyr. Hodell et al. (2017) obtained a comparable phase lead (6 kyr) for the ODP 1123 Mg/Ca record relative to eccentricity, after transferring a timescale matched to a southwest Iberian margin cores precession-based agemodel for the last 420 kyr. Shakun et al. 2015,

using a stack of planktonic foraminiferal $\delta^{18}\text{O}$ and SST records, found a range of lags of $\delta^{18}\text{O}_{\text{sw}}$ to sea surface temperature.

Ruddiman (2006; 2003) argued that such a slow reaction of the ice sheets would have ice sheets melting late into phases of glaciation, such as a substantial part of Marine Isotope Stage (MIS) 5. This argument appears to have been based on the premise that warming ahead of the deglaciation could be no earlier than the eccentricity minimum associated with the deglaciation. If true, this would have restricted the timing of ice melting in relation to the eccentricity minimum. He concluded that "Spectral analysis, cross-correlation analysis, and analysis of leads and lags on terminations all rule out the possibility that CO_2 leads ice volume by 12,000 years at the 100,000-year period, as proposed by Imbrie et al. (1993) and Shackleton (2000)" (Ruddiman, 2006, p48). If, as the Mg/Ca records suggest, there is a substantial phase lead of temperature to conventionally expressed orbital eccentricity, then temperatures in the deep ocean can begin to decline early in the interglacials, which removes this apparent paradox.

3.4 Carbon dioxide concentrations and deglaciations

Ruddiman (2006) also argued that the phase of CO_2 change documented in Antarctic ice cores was too close to that of deglacial sea level rise as indicated by coral records, for example from Barbados (Austerman et al. 2013) for the CO_2 changes to be driving the ice volume changes. He suggested that the CO_2 was instead responding in tandem to the ice volume changes, as a combined response and feedback to a process ultimately driven by ice sheet dynamics. An early phase of temperature change in relation to ice volume change is consistent with models – such as that described in this paper – that use combined eccentricity (ie use both increased intensity at high eccentricity perihelion and increased seasonal summer duration at low eccentricity states) to drive oceanic warming. Such a warming curve, in tandem with anti-phased precessional insolation gradients, would drive oceanic circulatory changes, ultimately resulting in CO_2 release. Deglaciation would then involve CO_2 as both a response and a positive-feedback forcing. The difference in emphasis is that the CO_2 change could also play a role in triggering deglaciation, with a very short reaction time of 1-2 kyr as observed in the ice sheet records. Although primed by oceanic temperature change shaped by the combined eccentricity forcing, the deglaciation was ultimately triggered by northern hemisphere insolation changes working together with oceanic CO_2 release, which changed air temperatures and was closely connected with oceanic circulation changes (Howe et al. 2016).

3.5 Precessional involvement in deglaciation

A phase lead of around 10,000 years might lead to a suspicion that the southern hemisphere precessional configuration was responsible for the temperature change, since the southern-hemisphere precessional forcing precedes northern-hemisphere precessional forcing by 10,000 years, or half a cycle. Two observations mitigate against this: the first is that Kawamura et al. (2007), using N/O ratios, demonstrated that Antarctic air temperatures were in phase with northern rather than southern hemisphere forcing. Huybers (2006) argued that southern hemisphere insolation duration may have been the relevant southern hemisphere forcing, but this would be in phase with northern hemisphere insolation intensity increases. The second problematic observation is that such forcing could not account for the remaining "out of phase" long-term sinusoidal component of the marine temperature record. As a driver of deglaciation, it could only explain the abrupt deglaciation itself, and would remain in conflict with the timescale of Kawamura et al. (2007). Since the amplitudes of precessional cycles, both north and south, are governed by the eccentricity cycle, it is difficult to explain a hard-hitting precessional cycle that "anticipates" an increase in the eccentricity value, although a growth-related increase in the vulnerability of the ice sheets might help (eg Abe-Ouchi et al. 2013).

An ingenious suggestion made by Rial (1995) was that the rate of change of insolation forcing, rather than the forcing itself, might be responsible for pacing the glacial-interglacial climatic changes. The first derivative of the insolation curve does indeed produce a saw-tooth that fits the climatic response well and has the required phase relationship to the response. However, the energetic changes associated with such changes are even smaller than those directly induced by insolation, as Rial acknowledged. More seriously, the upturn in the rate of change curve is not a "warming"; it is a decrease in the rate of cooling, something which seems unlikely in itself to bring about a dramatic warming. Rial subsequently developed an alternative hypothesis, arguing instead that control of the 100 kyr cycle by its more powerful amplitude modulation at 400 kyr periodicities (Rial 1999). There remain unresolved issues with the revised frequency modulation hypothesis. It is not clear how it could explain an early phase climatic response, particularly at 400 kyr intervals of strong eccentricity, where the amplitude modulation of eccentricity should be exercising closest control.

3.6 The combined eccentricity hypothesis

If the phase lead of deep ocean temperature to eccentricity is an accurate reflection of deep water

temperature variations, most of the existing models of the operation of the eccentricity cycle referred to in previous sections can be ruled out at a stroke, considerably narrowing the broad field of competing hypotheses.

Taking the two components of eccentricity - potential forcing by high and low eccentricity, insolation intensity and insolation seasonal duration - separately, it is apparent that if the climate system responded to the component forcings immediately and with equal effect, they would cancel each other out almost completely; the net insolation change associated with the eccentricity cycle is indeed very small. This, incidentally, is also true of the other two principle Milankovitch forcing periodicities, obliquity and precession, which always “balance” themselves annually at any particular latitude.

The suggestion of this paper is that the oceanic temperature response at the eccentricity periodicity may not have been initiated by the conventional (insolation intensity) eccentricity curve at a particular latitude and season, but by the much earlier phase combined eccentricity curve, which integrates both aspects of the eccentricity forcing but involves a very substantial lag to the inverse component of eccentricity (low eccentricity, with extended seasons). Such a parsing of the eccentricity related energy would enable the oceans to warm well ahead of the eccentricity intensity (and precessional/obliquity) forcings that drove the deglaciations, perhaps resolving the early phase problem (Fig. 8).

The two components of eccentricity - intensity and duration - are very different in nature and this could enable the climate system to respond to them in very different ways. For example, ice sheets are geographically relatively fixed in location and can essentially only respond to insolation changes by waxing or waning in volume and/or extent, and to some extent geographical shape, whereas the oceans redistribute energy between hemispheres and via interactions with the atmosphere, the growth and loss of sea ice, and other rapid processes.

The oceanic capacity for energetic redistribution provides the means both for energy redistribution and loss, but also for heat energy storage during episodes of oceanic stratification. An extension of the duration of the warm season lends itself to the storage of heat by a stratified glacial ocean, a cumulative warming effect with a potentially long lag. The resumption of stratification would be accompanied by an initial cooling of the deep ocean, maintaining the lead of oceanic temperatures over ice volume. A “stored” oceanic heat reservoir – of the order of half a degree to one degree centigrade – would have a

profound effect on global climate if released into the atmosphere at a time of a warming instability in the Northern hemisphere precessional cycle. Salinity stratification of the ocean during the glacials would be a prerequisite of heat accumulation in intermediate or deep water masses. The warmer water would be formed at lower latitudes than during glacials and the additional heat would derive from the extended summers of low eccentricity states. In a stratified ocean, it is also possible that geothermal sources would make a contribution to enhanced heat storage by the oceans, but we favour the inverse eccentricity model because of its precise match to the residual from “standard” eccentricity (Fig. 8).

An extended moderately warm summer (low eccentricity) would be unlikely to have a significant melting effect on an ice sheet, since the ice sheet is protected by its albedo - and in the case of Antarctica, thermal isolation by the powerful Antarctic Circumpolar Current. Instead, ice would continue to accumulate, even though some parts of the deep sea were warming, as the Mg/Ca record indicates (Sosdian and Rosenthal, 2009; Elderfield et al, 2012). When a higher eccentricity state develops higher insolation intensity at perihelion in summer, passing Huyber and Denton’s (2008) “cumulative insolation” threshold, this aspect of forcing, combined with the previously accumulated oceanic warming, would perhaps be enough to bring about deglaciation, in part by destabilising the stratified ocean and releasing the heat and CO₂ stored in it.

From this point of view the higher insolation intensity at the two poles, although switching between the poles depending on the precessional state, can be regarded as a single high eccentricity forcing component, equivalent to the upper amplitude envelope of precession. A higher amplitude of precession will enhance the seasonal thermal gradients between the poles, inducing a more energetic oceanic circulation.

In contrast, ice sheets - and in particular the largely land-surrounded northern ice sheet - are only able to respond to an excessive warming, by melting. During low eccentricity states, in which both hemispheres experience extended summers, the redistribution of heat by the oceans results in a net warming of the deep ocean, even during glacial stages (times of high ice volume). Precipitation, and the resulting ice-sheet mass accumulation, continue. When eccentricity is high, and the northern ice sheet is exposed to an intense warming because the precessional state puts northern summer at perihelion, a combined insolation/oceanic warming threshold is crossed. The ice sheet (which at this point is at a lower elevation due to its cumulative mass, as Abe-Ouchi et al. 2013 point out) is exposed to a

pre-warmed ocean, and catastrophic deglaciation follows.

Because the mechanism proposed here is bound up with the size and behaviour of ice sheets, the question of the initiation of 100 kyr cyclicity as the dominant climate cycle after the Mid-Pleistocene transition becomes easier to resolve. At MIS 22 an accumulation of an anomalously large quantity of ice - ultimately resulting from the long-term decline in CO₂ levels - switched the climate system into a combined ice-ocean response, in contrast to the largely oceanically controlled 41 kyr world that preceded it. The effect of the combined eccentricity curve - an eccentricity "double punch" - produced the catastrophic Late Pleistocene deglaciations that locked global climatological responses into a 100 kyr cyclicity, up to the point at which anthropogenic forcings began to override natural forcings (Tzedakis et al. 2012).

In order to test the compatibility of such a forcing with the overall climatic response documented by benthic $\delta^{18}\text{O}$ record, we combined the orbital forcing components which are believed to be better understood and more linearly related to global climate behavior – obliquity and precession – with the combined eccentricity curve using the relative amplitudes suggested by the spectral analysis of the benthic $\delta^{18}\text{O}$ record from ODP 1123. Fig. 9 shows that, with the other orbital components scaled according to their associated climatic response, combined eccentricity, obliquity and precession can account for the observed benthic $\delta^{18}\text{O}$ record with appropriate phases; in effect a linear response to the climate forcing, to the extent that the combined eccentricity model can be considered “linear”.

Fig. 10 shows that the combined eccentricity forcing curve has a single spectral peak at almost exactly 100 kyr, and has almost no component at 400 kyr, a characteristic that has been highlighted, among others, as requiring explanation (Muller and McDonald 2000). The combined eccentricity forcing/pacing also shows effectively zero lag for the ODP 1123 benthic temperature curve, using equal proportions of normal and inverse eccentricity and a 26 kyr lag for the inverse component. Such a lag is inferred from the phase offset, but would be consistent with a linear but slow response time of the reservoir (in this case, the ocean/ice system) relative to the forcing (in this case, orbitally induced insolation changes). Other climate proxies might require slightly different lags or different inverse components to explore possible relationships to combined eccentricity, but the equal proportions and 26 kyr lag suggest useful first order quantities for the mix.

4. Conclusion

The degree of alteration required to produce the observed phase lead by a carbonate ion effect, either during calcification or by dissolution, would require the carbonate ion effect to be significantly greater than currently estimated for infaunal species (Elderfield et al. 2006). The timing of change in carbonate ion concentrations is therefore difficult to reconcile with the observed Mg/Ca temporal relationship to eccentricity.

Several of the difficulties associated with the pacing - or even forcing - of the climate by the orbital eccentricity cycle can be resolved by assuming a long-lagged, cumulative contribution from low eccentricity ("inverse eccentricity") to the Earth's climatic state, via long term storage of heat in the oceans during glacial stages. The narrow 100 kyr periodicity of the signal, the absence of a 400,000 year spectral component, the phase relationship to climatic changes, and the energetic budget associated with the cycle can apparently be resolved in this way. The change of pace from a dominantly 41 kyr regime to a 100 kyr regime at the Mid Pleistocene Transition becomes easier to understand, since the climatic response to the eccentricity cycle involves both large ice sheets and oceanic circulation. Ice sheets reach new volumetric maxima at the time of the mid-Pleistocene transition, creating a robust combined oceanic-ice sheet 100 kyr climate regime. Harry Elderfield's deconvolution of temperature and ice volume by means of magnesium/calcium ratios in benthic foraminifera continues to suggest possible insights towards understanding the behaviour of the climate system, and its subtle but remarkably powerful relationship with orbital forcing.

Acknowledgements

This paper was greatly improved by discussions with Harry Elderfield, David Hodell, Della Murton, Alex Piotrowski, Heather Ford and Nick McCave. The reviewers were exceptionally thoughtful and helpful, and we only hope that we have done their comments justice. Tom Marchitto patiently and constructively guided us to the completion of the manuscript. The ODP 1123 benthic isotope and Mg/Ca records were the product of a vast amount of work by Harry Elderfield, Mervyn Greaves, Patrizia Ferretti, Linda Booth, Caroline Daunt and others at the Godwin Institute for Quaternary Research in Cambridge. This research did not receive any specific grant from funding agencies in the public, commercial, or not-for-profit sectors.

References

- Abe-Ouchi A., Saito F., Kawamura, K., Raymo M. E., Okuno J., Takahashi K. and Blatter H. (2013) Insolation-driven 100,000-year glacial cycles and hysteresis of ice-sheet. *Nature* **500**, 190–193.
- Austermann J., Mitrovica J. X., Latychev K., and Milne G. A. (2013) Barbados-based estimate of ice volume at Last Glacial Maximum affected by subducted plate. *Nat. Geosci.* **6**, 553–557.
- Broecker W. S. and Henderson G. M. (1998) The sequence of events surrounding Termination II and their implications for the cause of glacial-interglacial CO₂ changes. *Paleoceanography* **13**, 352–364.
- Broecker W. & Yu J. 2011, 'What do we know about the evolution of Mg to Ca ratios in seawater?', *Paleoceanography*, **26**, no. 3.
- Crosta, X., Pichon, J.-J. and Burckle, J.-J. (1998) Reappraisal of Antarctic seasonal sea-ice at the Last Glacial Maximum. *Geophysical Research Letters* **25**, no. 14, 2703–2706.
- Crundwell M. P., Scott G. H., Naish T. R. and Carter L. (2008) Glacial-interglacial ocean climate variability from planktonic foraminifera during the Mid-Pleistocene transition in the temperate Southwest Pacific, ODP Site 1123. *Palaeogeography, Palaeoclimatology, Palaeoecology*, **260**(1–2), 202–229.
- Ditlevsen P. D. (2009) Bifurcation structure and noise-assisted transitions in the Pleistocene glacial cycles. *Paleoceanography* **24**, PA3204 doi:10.1029/2008PA001673.
- Elderfield H., Ferretti P., Greaves M., Crowhurst S., McCave I. N., Hodell D., and Piotrowski A. M. (2012) Evolution of ocean temperature and ice volume through the Mid-Pleistocene climate transition. *Science* **337**, 704–709.
- Elderfield H., Greaves M., Barker S., Hall I. R., Tripathi A., Ferretti P., Crowhurst S., Booth L., and Daunt C. (2010) A record of bottom water temperature and seawater $\delta^{18}\text{O}$ for the Southern Ocean over the past 440 ka based on Mg/Ca of benthic foraminiferal *Uvigerina* spp. *Quat. Sci. Rev.* **29**, 160–169.
- Elderfield, H., Yu, J., Anand, P., Kiefer, T., Nyland, B. (2006) Calibrations for benthic foraminiferal Mg/Ca paleothermometry and the carbonate ion hypothesis. *Earth and Planetary Science Letters*, **250**, Issue 3–4, 633–649.
- Elmore A. C., McClymont E. L., Elderfield H., Kender S., Cook M. R., Leng M. J., Greaves M. J. and Misra S. (2015) Antarctic Intermediate Water properties since 400 ka recorded in infaunal (*Uvigerina peregrina*) and epifaunal (*Planulina wuellerstorfi*) benthic foraminifera. *Earth and Planetary Science Letters* **428**, 193–203.
- Freeman E., Skinner L. C., Waelbroeck C., and Hodell D., 2016. Radiocarbon evidence for enhanced respired carbon storage in the Atlantic at the Last Glacial Maximum. *Nature Commun.* **7**:11998
- Gradstein F.M., Ogg J.G., Schmitz M.D., and Ogg G.M., eds, (2012) *The Geological Time Scale 2012*, Elsevier, Amsterdam, 2 vols., 1144 p. Ch 4, Cyclostratigraphy and Astrochronology.
- Hays J.D., Imbrie J. and Shackleton N.J. (1976) Variations in the Earth's orbit: Pacemaker of the Ice Ages *Science*, **194**, 1121–1132.
- Hilgen F. J. (1991a) Astronomical calibration of Gauss to Matuyama sapropels in the Mediterranean and implication for the geomagnetic polarity time scale. *Earth Planet. Sci. Lett.* **104**, 226–244.

Hilgen F. J. (1991b). Extension of the astronomically calibrated (polarity) time scale to the Miocene Pliocene boundary. *Earth Planet. Sci. Lett.* **107**, 349–368.

Hodell, D., Crowhurst, S., Skinner, L. Tzedakis, P.C., Margari, V., Channell, J.E.T., Kamenov, G., Maclachlan, S., and Rothwell, G. (2017) Response of Iberian Margin sediments to orbital and suborbital forcing over the past 420 ka. *Paleoceanography* **28**, 185 – 199

Hodell D., Lourens L., Crowhurst S., Konijnendijk T., Tjallingii R., Jiménez-Espejo F., Skinner L., Tzedakis, P. C. and Members, S. S. P. (2015) A reference time scale for Site U1385 (Shackleton Site) on the SW Iberian Margin. *Glob. Planet. Chang.* **133**, 49–64.

Howe J. N. W., Piotrowski A. M., Oppo D. W., Huang K.-F., Mulitza S., Chiessi C. M. and Blusztajn J. (2016) Antarctic intermediate water circulation in the South Atlantic over the past 25,000 years *Paleoceanography* **31**, 1302–1314.

Huybers P. (2006) Early Pleistocene Glacial Cycles and the Integrated Summer Insolation Forcing. *Science*, **313**, 508-511.

Huybers P. (2007) Glacial variability over the last 2Ma: an extended depth-derived age model, continuous obliquity pacing, and the Pleistocene progression. *Quat. Sci. Rev.* **26**, 37–55.

Huybers P. and Denton G. (2008) Antarctic temperature at orbital timescales controlled by local summer duration. *Nat. Geosci.* **1**, 787-792.

Imbrie J., Berger A., Boyle E. A., Clemens S. C., Duffy A., Howard W. R., Kukla G., Kutzbach J., Martinson D. G., McIntyre A., Mix A. C., Molfino B., Morley J. J., Peterson L. C., Pisias N. G., Prell W. L., Raymo M. E., Jaccard S. L., Galbraith E. D., Martínez-García A., and Anderson R. F. (2016) Covariation of deep Southern Ocean oxygenation and atmospheric CO₂ through the last ice age. *Nature* **530**, 207–210.

Jahnke, R.A. and Jahnke, B.J. (2004) Calcium carbonate dissolution in deep sea sediments: Reconciling microelectrode, pore water and benthic flux chamber results. *Geochimica et Cosmochimica Acta* **68**, 47-59.

Jouzel J., Masson-Delmotte V., Cattani O., Dreyfus G., Falourd S., Hoffmann G., Minster B., Nouet J., Barnola J.-M., Chappellaz J., Fischer H., Gallet J. C., Johnsen S. J., Leuenberger M., Loulergue L., Luethi D., Oerter H., Parrenin F., Raisbeck G. M., Raynaud D., Schilt A., Schwander J., Selmo E., Souchez R., Spahni R., Stauffer B., Steffensen J. P., Stenni B., Stocker T. F., Tison J.-L., Werner M., Wolff E. W. (2007): Orbital and millennial Antarctic climate variability over the past 800,000 years. *Science*, **317**(5839), 793-797.

Kawamura K., Parrenin F., Lisiecki L., Uemura R., Vimeux F., Severinghaus J. P., Hutterli M. A., Nakazawa T., Aoki S., Jouzel J., Raymo M. E., Matsumoto K., Nakata H., Motoyama H., Fujita S., Goto-Azuma K., Fujii Y., and Watanabe, O. (2007) Northern Hemisphere forcing of climatic cycles in Antarctica over the past 360,000 years. *Nature* **448**, 912-916.

Kerr J., Rickaby R. E. M., Yu J., Elderfield H. and Sadekov, A. (2017). The effect of ocean alkalinity and carbon transfer on deep-sea carbonate ion concentration during the past five glacial cycles. *Earth and Planetary Science Letters*, 471, 42-53.

Kostadinov T.S. and Gilb, R. (2014) Earth Orbit v2.1: a 3-D visualization and analysis model of Earth's orbit, Milankovitch cycles and insolation. *Geosci. Model Dev.*, **7**, 1051-1068.

Laskar J. (1990) The chaotic motion of the solar system: A numerical estimate of the size of the chaotic zones *Icarus*, **88**, 266-291.

- Laskar J., Fienga A., Gastineau M., and Manche, H. (2011) La2010: A new orbital solution for the long term motion of the Earth. *Astron. Astrophys.* **A89**, doi: 10.1051/0004-6361/201116836.
- Laskar J., Robutel P., Joutel F., Gastineau M., Correia A. C. M., and Levrard B. (2004) A long term numerical solution for the insolation quantities of the Earth. *Astron. Astrophys.* **428**, 261-285.
- Lear, C. H., Elderfield, H., and Wilson, P.A. (2000) Cenozoic deep-Sea temperatures and global ice volumes from Mg/Ca in benthic foraminiferal calcite *Science* **287(5451)**, 269-272.
- Liebrand D., Beddow H. M., Lourens L. J., Pälike H., Raffi I., Bohaty S. M., Hilgen F. J., Saes M. J. M., Wilson P. A., and Dijk, A. E. (2016) Cyclostratigraphy and eccentricity tuning of the early Oligocene through early Miocene (30.1-17.1 Ma): *Cibicides mundulus* stable oxygen and carbon isotope records from Walvis Ridge Site 1264. *Earth Planet. Sci. Lett.* **450**, 392–405.
- Lisiecki L. E. (2010) Links between eccentricity forcing and the 100,000-year glacial cycle. *Nature Geoscience* . **3**, 349-352.
- Lisiecki L. E., and Raymo M.E. (2005) A Pliocene-Pleistocene stack of 57 globally distributed benthic $\delta^{18}\text{O}$ records. *Paleoceanography* **20** PA1003.
- Lüthi D., Le Floch M., Bereiter B., Blunier T., Barnola J.M., Siegenthaler, U. Raynaud, D. Jouzel J., Fischer H., Kawamura K. and Stocker T.F. (2008). High-resolution carbon dioxide concentration record 650,000-800,000 years before present. *Nature*, **453**, 379-382.
- Marcott S. A., Clark P. U., Padman L., Klinkhammer G. P., Springer S. R., Liu Z., Otto-Bliesner B. L., Carlson A. E., Ungerer A., Padman J., He F., Cheng J., and Schmittner A. (2011) Ice-shelf collapse from subsurface warming as a trigger for Heinrich events. *Proc. Nat. Acad. of Sci.* **108**, 13415–13419.
- Matteucci G. (1989) Orbital forcing in a stochastic resonance model of the Late-Pleistocene climatic variations. *Climate Dynamics*, **3**, Issue 4, 179–190.
- Muller R. and MacDonald G.J. (2000) *Ice ages and Astronomical causes: data, spectral analysis and mechanisms*. Springer, London.
- Paillard, D., Labeyrie, L., and Yiou (1996) Macintosh Program performs time-series analysis *EOS Trans* **77**, 379.
- Raymo M. E., Lisiecki L. E., and Nisancioglu K. H. (2006) Plio-Pleistocene Ice Volume, Antarctic Climate, and the Global $\delta^{18}\text{O}$ Record. *Science* **313**, 492–495.
- Rial J. A. (1995) On the origin of the long period sawtooth shape of the Late Pleistocene paleoclimate records: the first derivative of the Earth's orbital eccentricity. *Geophys. Res. Lett.* **22**, 1997–2000.
- Rial J. A. (1999) Pacemaking the ice ages by frequency modulation of Earth's orbital eccentricity. *Science* **285**, 564–568.
- Ruddiman W.F. (2003) Orbital insolation, ice volume, and greenhouse gases. *Quaternary Science Reviews* **22**, 1597–1629.
- Ruddiman W. F. (2006) Ice-driven CO_2 feedback on ice volume. *Clim. Past* **2**, 43-55.
- Shackleton N. J. (2000) The 100,000 year Ice-Age cycle identified and found to lag temperature, carbon dioxide and orbital eccentricity. *Science* **289**, 1897–1902.
- Shackleton, N. J. and Toggweiler, J. R. (1993) On the structure and origin of major glaciation cycles 2. The 100,000-year cycle. *Paleoceanography* **8**, 699–735.

- Shakun J.D., Lea D.W., Lisiecki L.E. and Raymo M.E. (2015) An 800-kyr record of global surface ocean $\delta^{18}\text{O}$ and implications for ice volume-temperature coupling. *Earth and Planetary Science Letters*, **426** 58–68.
- Sosdian S. and Rosenthal Y. (2009) Deep-sea temperature and ice volume changes across the Pliocene-Pleistocene climate transitions. *Science* **325**, 306–310.
- Sosdian S. and Rosenthal Y. (2010) Response to Comment on “Deep-Sea Temperature and Ice Volume Changes Across the Pliocene-Pleistocene Climate Transitions” *Science*, **328**, 1480.
- Stephens B.B. and Keeling, R.F. (2000) The influence of Antarctic sea ice on glacial–interglacial CO_2 variations. *Nature* **404**, 171–174
- Stott L., A. Timmermann A. and Thunell R. (2007): Southern Hemisphere and deep-sea warming led deglacial atmospheric CO_2 rise and tropical warming. *Science*, **318**, 435–438.
- Thomas A. L., Henderson G. M., Deschamps P., Yokoyama Y., Mason A. J., Bard E., Hamelin B., Durand N., and Camoin G. (2009) Penultimate deglacial sea-level timing from Uranium/Thorium dating of Tahitian corals. *Science* **324**, 1186–1189.
- Tzedakis P. C., Channell J. E. T., Hodell D. A., Kleiven H. F., and Skinner L. C. (2012) Determining the natural length of the current interglacial. *Nat. Geosci.* **5**, 138–141.
- Yu J. and Broecker W. (2010) Comment on “Deep-Sea Temperature and Ice Volume Changes Across the Pliocene-Pleistocene Climate Transitions”, *Science*, **328**, 1480.
- Zeebe R.E and Marchitto T.M. (2010) Glacial cycles: Atmosphere and ocean chemistry *Nat. Geosci.* **3**, 386 - 387

Figure captions

Figure 1: Distribution of energy across the year at 65°N, illustrated by Earth_Orbit_v2.1 (Kostadinov and Gilb 2014); at 100 kyr periodicities the energy supplied at medium-low latitudes is consistently high over summer. At high eccentricities, insolation intensity is antiphased between hemispheres by orbital precession, motivating oceanic circulation; at low eccentricities, it is more evenly distributed between hemispheres.

Figure 2: The classic eccentricity problem: while the climate responses at obliquity and precessional frequencies can be explained as linear responses to orbital forcing, the 100 kyr climate cycles post-MPT (pink line, benthic O18 at ODP 1123, Elderfield et al. 2012) are disproportionately large relative to conventionally expressed eccentricity forcing, represented by insolation increases at particular latitudes at periodicities of around 100 kyr (blue line, insolation 65°N).

Figure 3: Cartoon (not to scale) illustrating the effects of Kepler’s second law: the time spent at perihelion is shortened at high eccentricity orbital states.

Figure 4: The temperature (panel A) and “ice volume” (deconvolved sea water $\delta^{18}\text{O}$) (panel B) components of the benthic $\delta^{18}\text{O}$ record from ODP 1123, shown in relation to the calcite $\delta^{18}\text{O}$ record from the site (from Elderfield et al. 2012).

Figure 5: Normalised and summed conventional orbital parameters (ETP based on Laskar 1990) filtered

at the 100 kyr periodicity (.01 kyr central frequency) in relation to the temperature component (Mg/Ca) of the ODP 1123 record (Elderfield et al. 2012; based on the LR04 benthic oxygen isotope stack timescale). The strong phase lead of the Mg/Ca record on the LR04 timescale after 800 kyr is apparent. For the LR04 timescale, see Lisiecki and Raymo 2005.

Figure 6: Spectral analysis of the composite EDC3 CO₂ record (Lüthi et al. 2008) and its phase relationship with orbital eccentricity (Laskar, 90). The spectral peak of orbital eccentricity (not shown) is slightly offset from that of the CO₂ record at the 100 kyr period, as shown for IODP 1123 Mg/Ca in Fig. 10. Coherence at this periodicity is well above the 90% confidence interval (coherence at 100 kyr=0.94; 90% confidence limit 0.52). Analyseries software used (Paillard et al. 1996).

Figure 7: A) The ODP 1123 Mg/Ca record synchronised with the EDC3 CO₂ record (Lüthi et al. 2008, available from the WDC at Boulder) using the Crundwell SST dataset for ODP 1123 (Crundwell et al. 2008, available from the Pangaea database) and the Deuterium ratio dataset for EDC/Antarctica (Jouzel et al., 2007, available from the Pangaea database). The combined CO₂ sequence has a smaller (half amplitude), inverted and 10kyr lagged additional CO₂ sequence combined with it to calibrate a potential carbonate ion distortion of the Mg/Ca sequence. A very significant carbonate ion contribution relative to atmospheric CO₂ variations, and a substantial phase lag (~10kyr) for the CO₂ induced carbonate ion effect are required if carbonate ion variations due to atmospheric CO₂ are responsible for the observed phase offset. Panel B) shows the spectral analysis of the combined CO₂ sequence, with its 9 kyr phase lead.

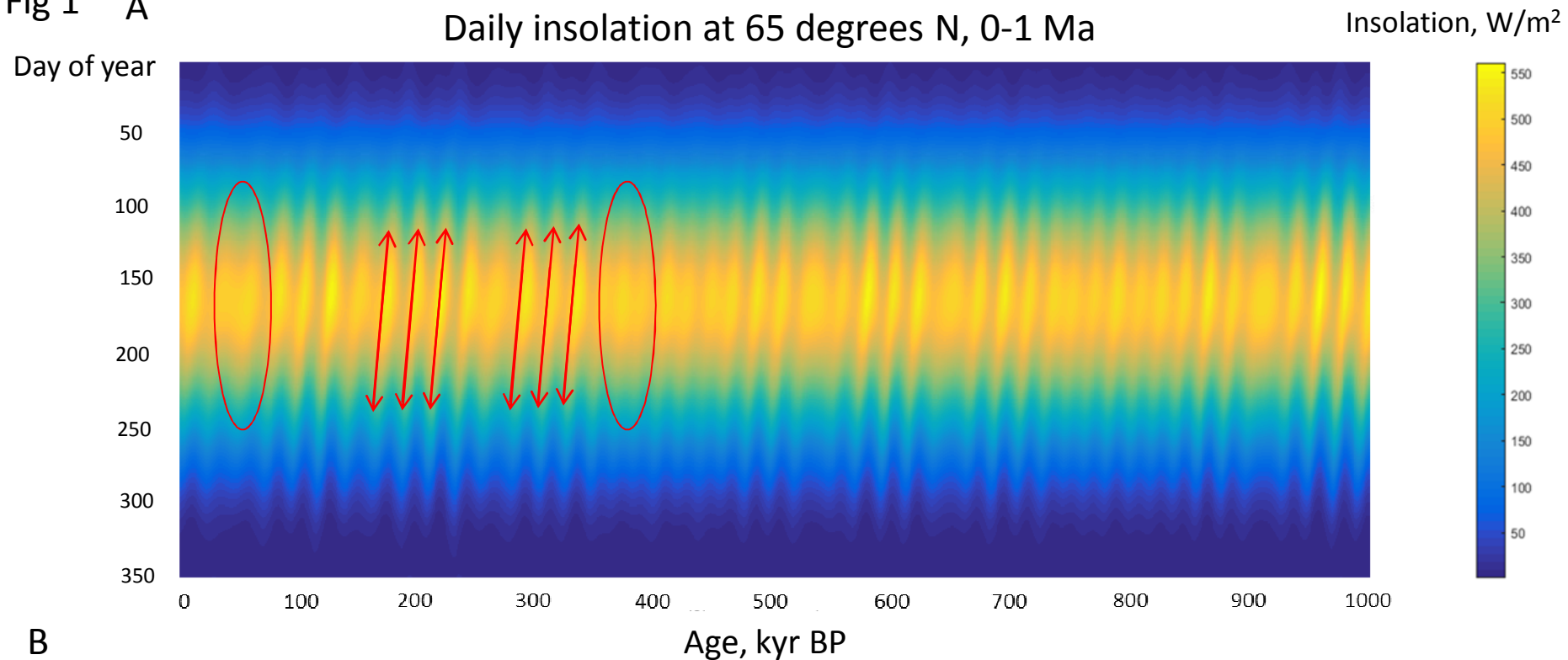
Figure 8: Linear spectrum of the combined eccentricity sequence in relation to 800 kyr of the ODP 1123 Mg/Ca temperature record (Elderfield et al. 2012). This figure illustrates how the lagged inverse eccentricity sequence complements the standard eccentricity sequence (Laskar 1990) in accounting for the 100 kyr variance in the ODP 1123 Mg/Ca record. The ODP 1123 Mg/Ca record was Gaussian interpolated with a 5 kyr gaussian window to 1 kyr intervals. Analyseries software used for spectral analysis (Paillard et al. 1996).

Figure 9: Combined eccentricity, obliquity and precession in relation to the total benthic $\delta^{18}\text{O}$ record from ODP 1123 (Elderfield et al. 2012). Mean amplitudes of components in the forcing/pacing model are taken from their mean amplitude in the benthic $\delta^{18}\text{O}$ curve. The figure illustrates that the benthic $\delta^{18}\text{O}$ record can be largely explained as a linear response to combined eccentricity, obliquity and precession, with appropriate linear scaling of the forcing components.

Figure 10: A comparison of the spectral power, coherence and phase of the standard eccentricity (Laskar 1990; panel A) and combined eccentricity (panel B) curves in relation to the ODP 1123 Mg/Ca (Elderfield et al. 2012) temperature record. Eccentricity components were normalised, and the 1123 Mg/Ca record put through a 5-kyr Gaussian window interpolation onto 1 kyr intervals. Small gaps in the interpolated sequence (less than 3%) were supplied by linear interpolation. The combined eccentricity shows strong

focusing at 100 kyr and little power at 400 kyr.

Fig 1 A



B

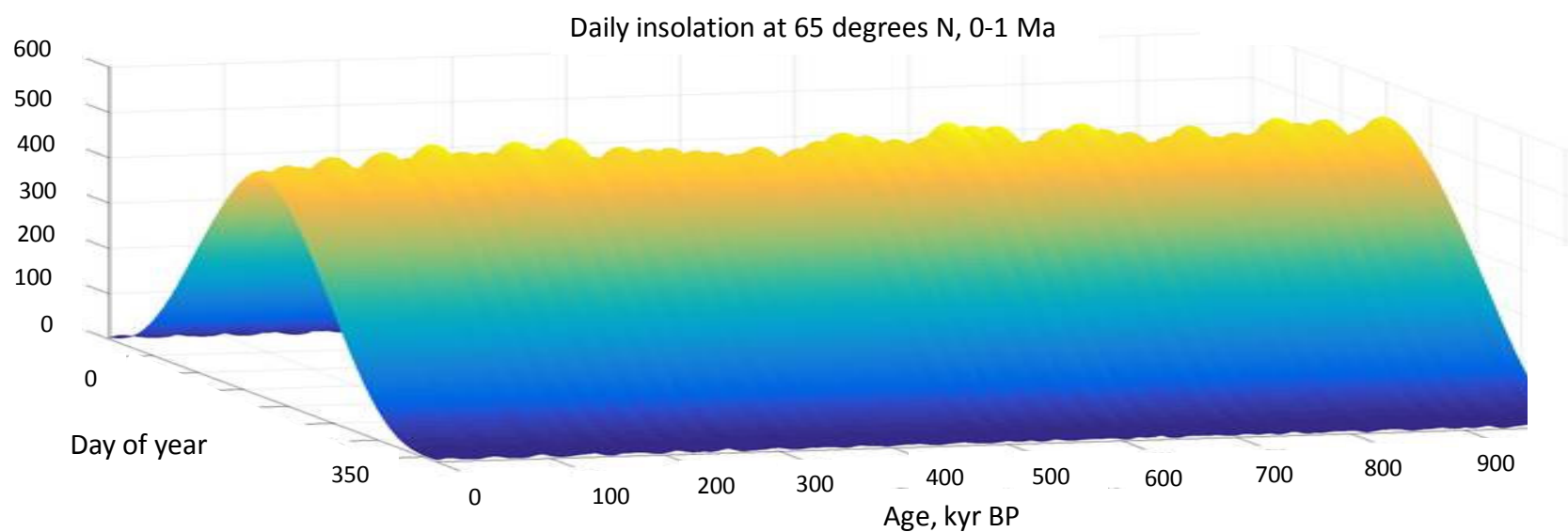


Fig 2

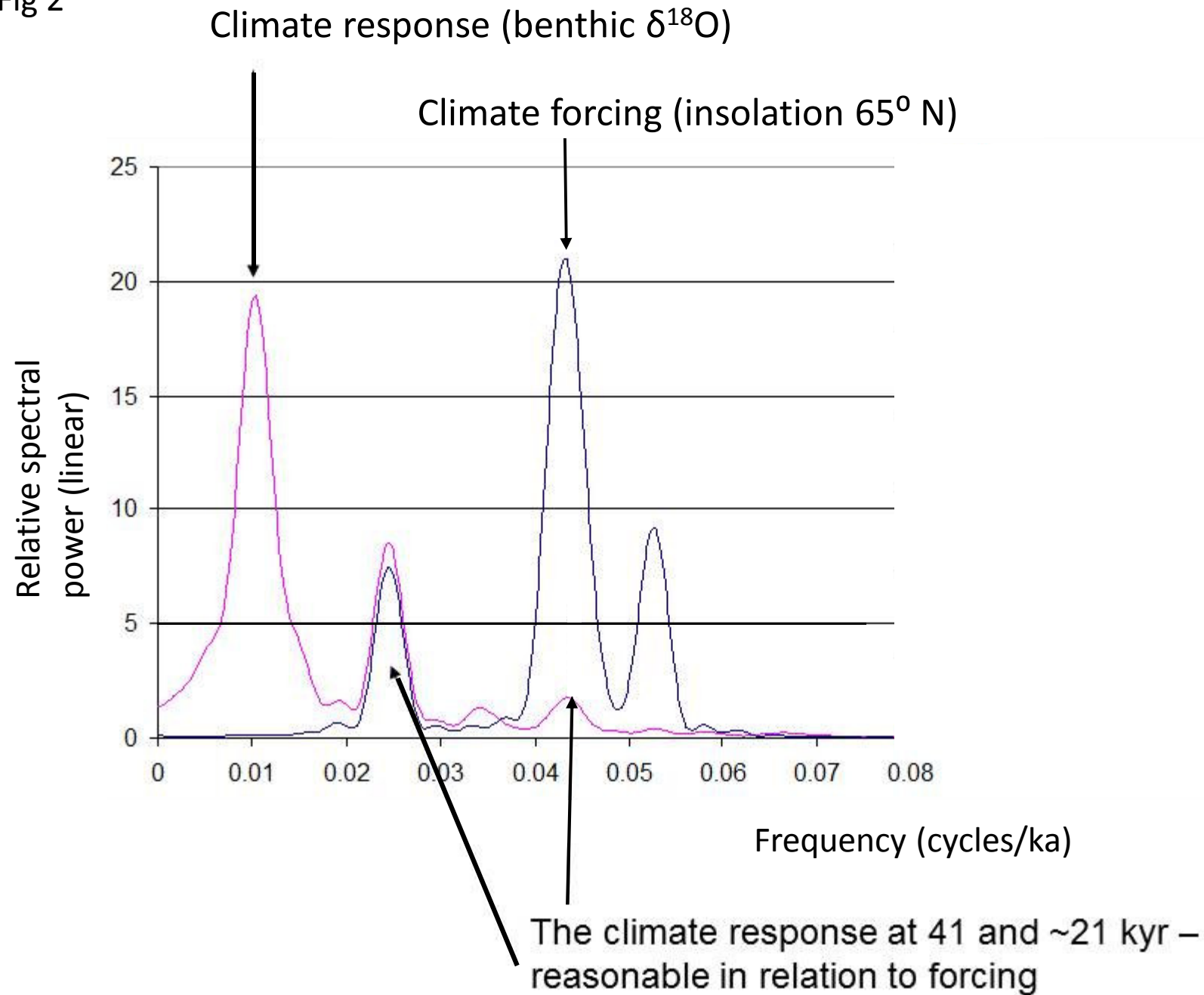


Fig 3

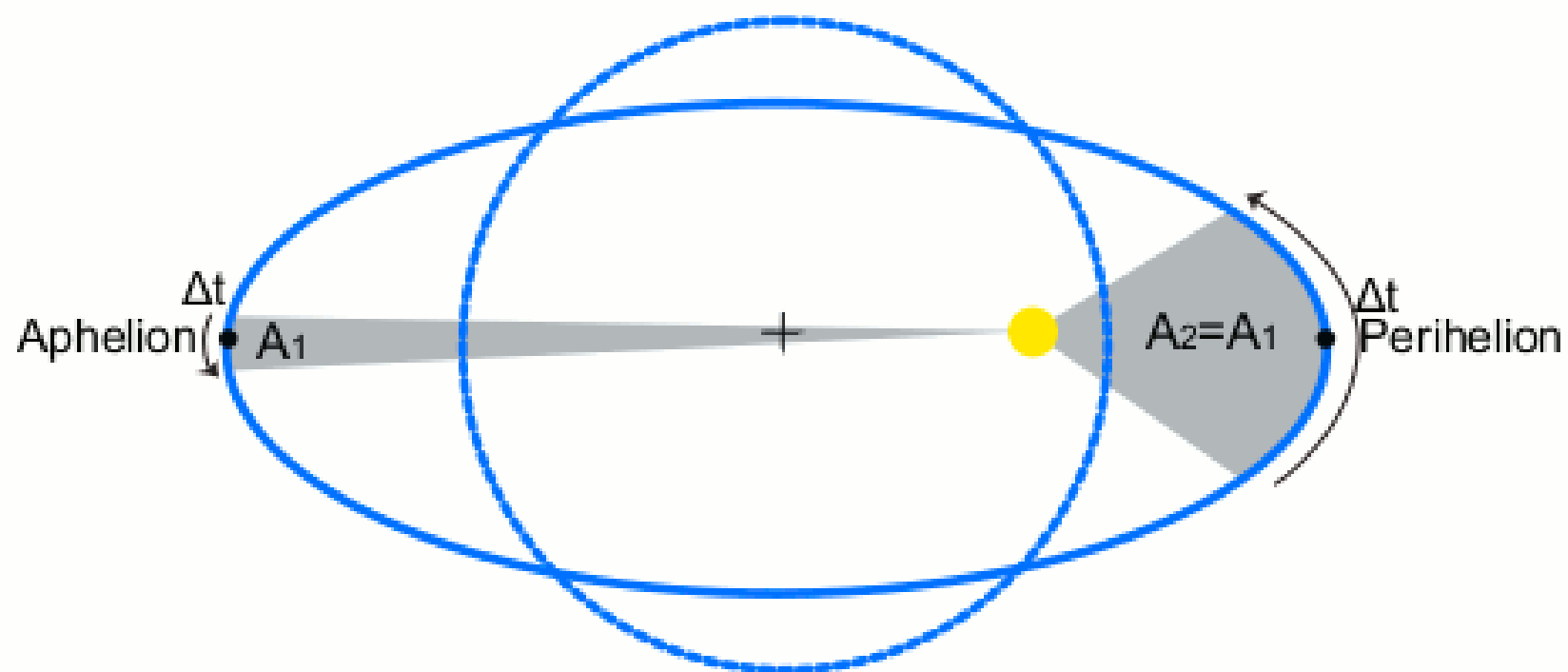


Fig 4

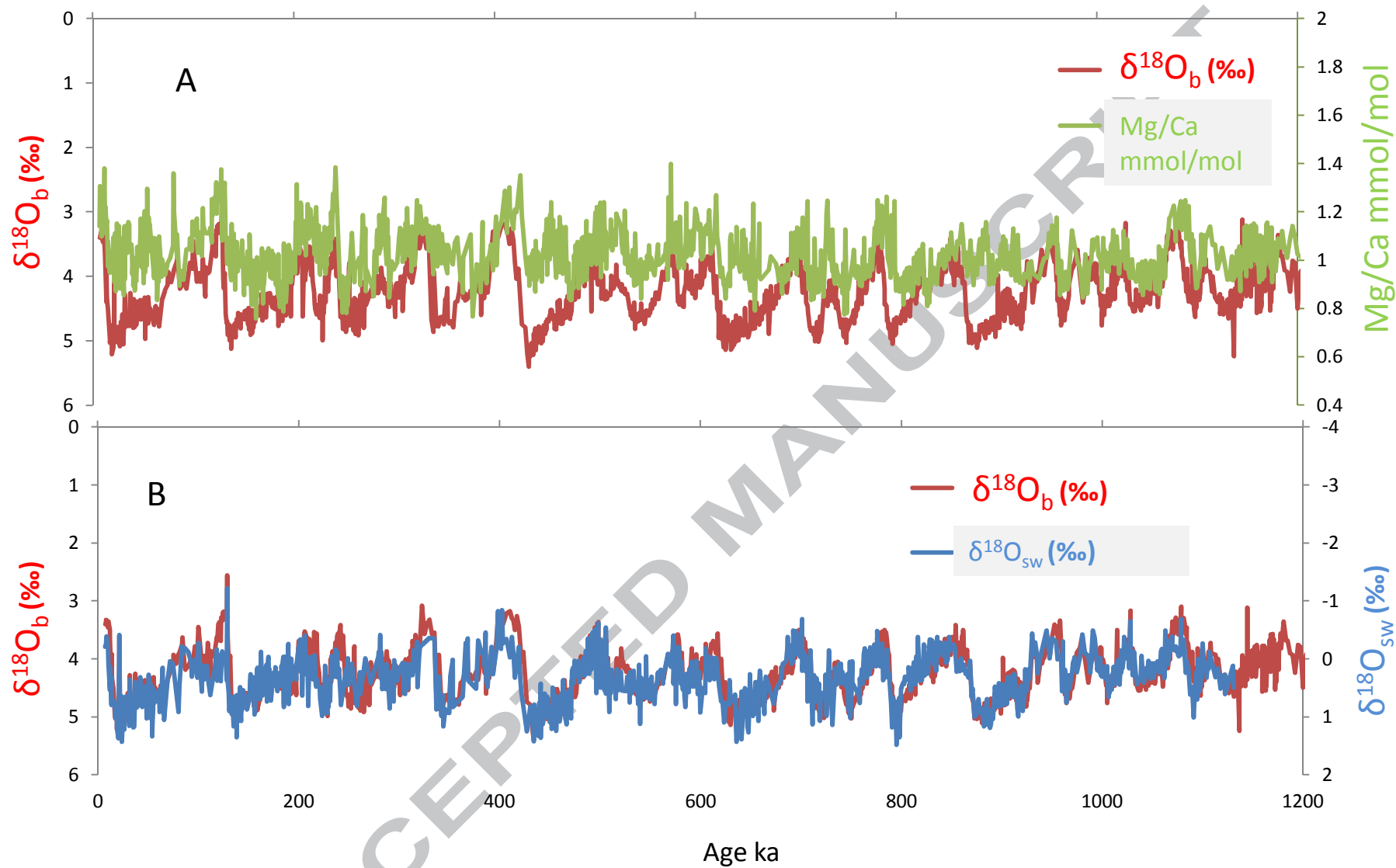


Fig 5

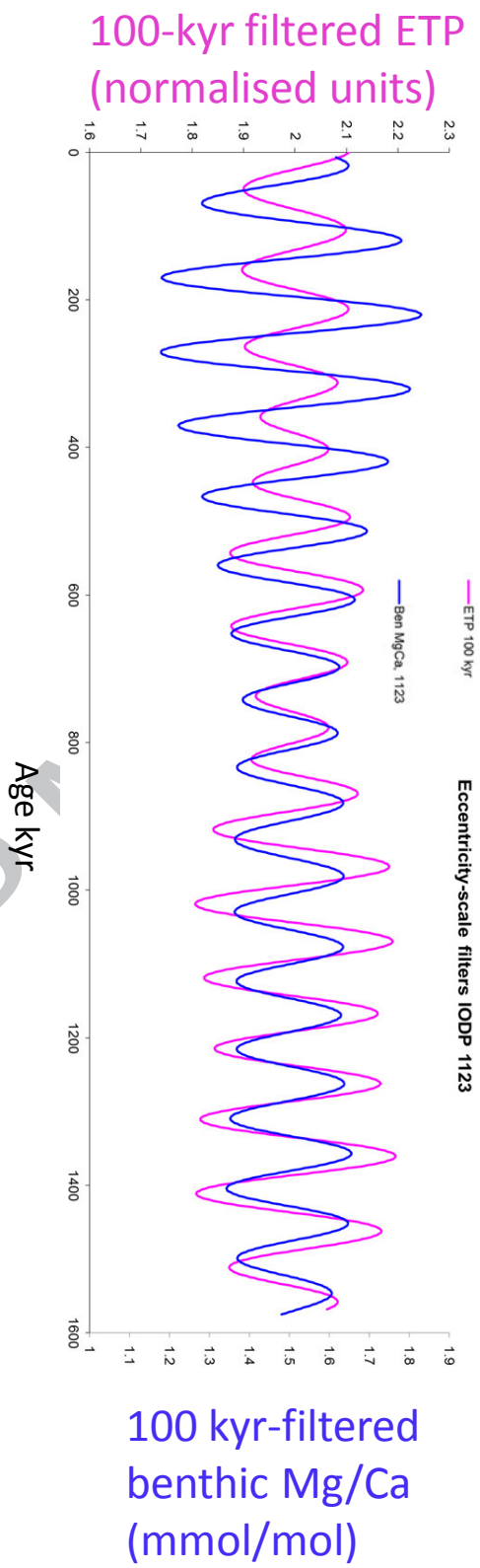


Fig 6

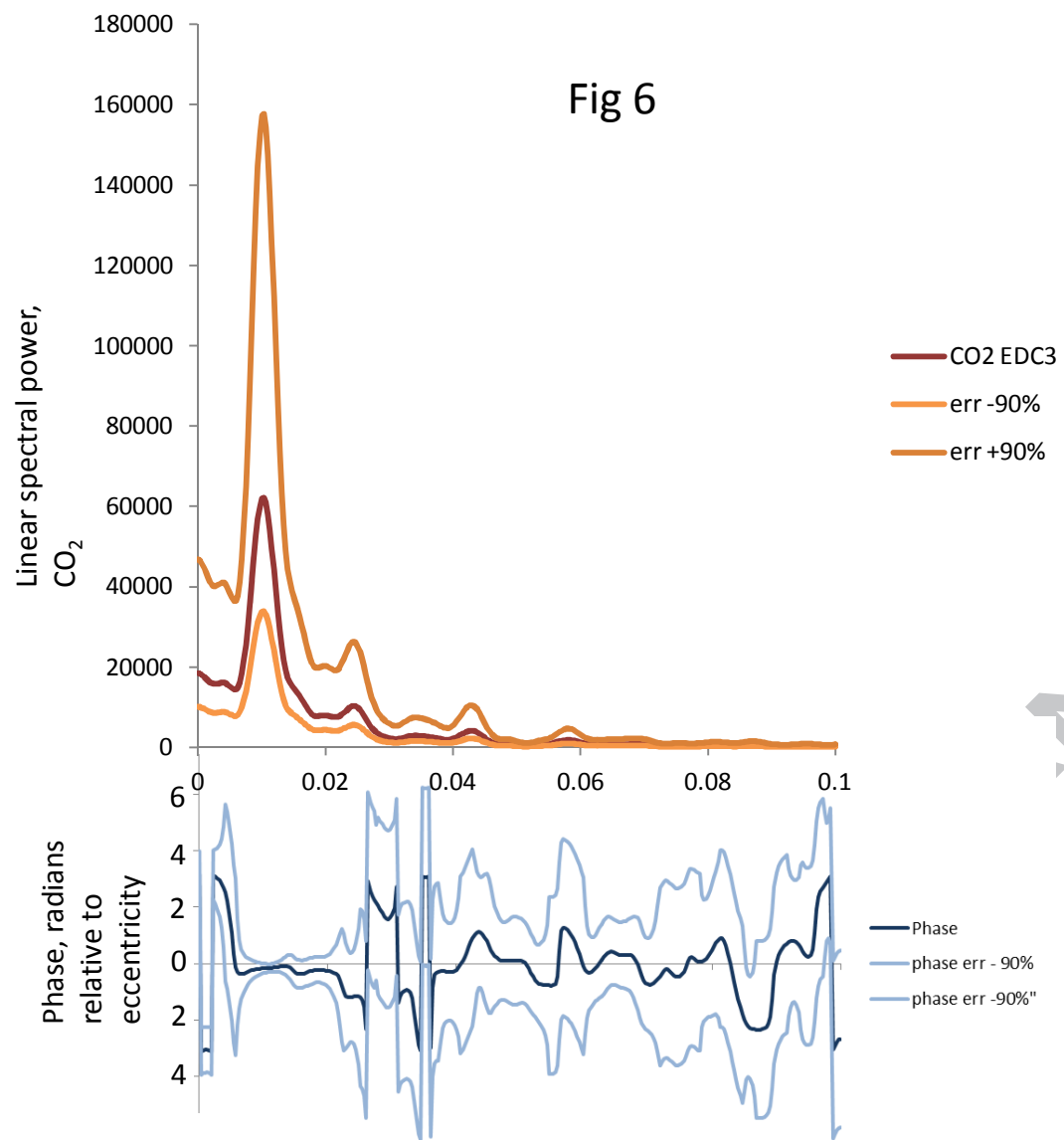


Fig 7

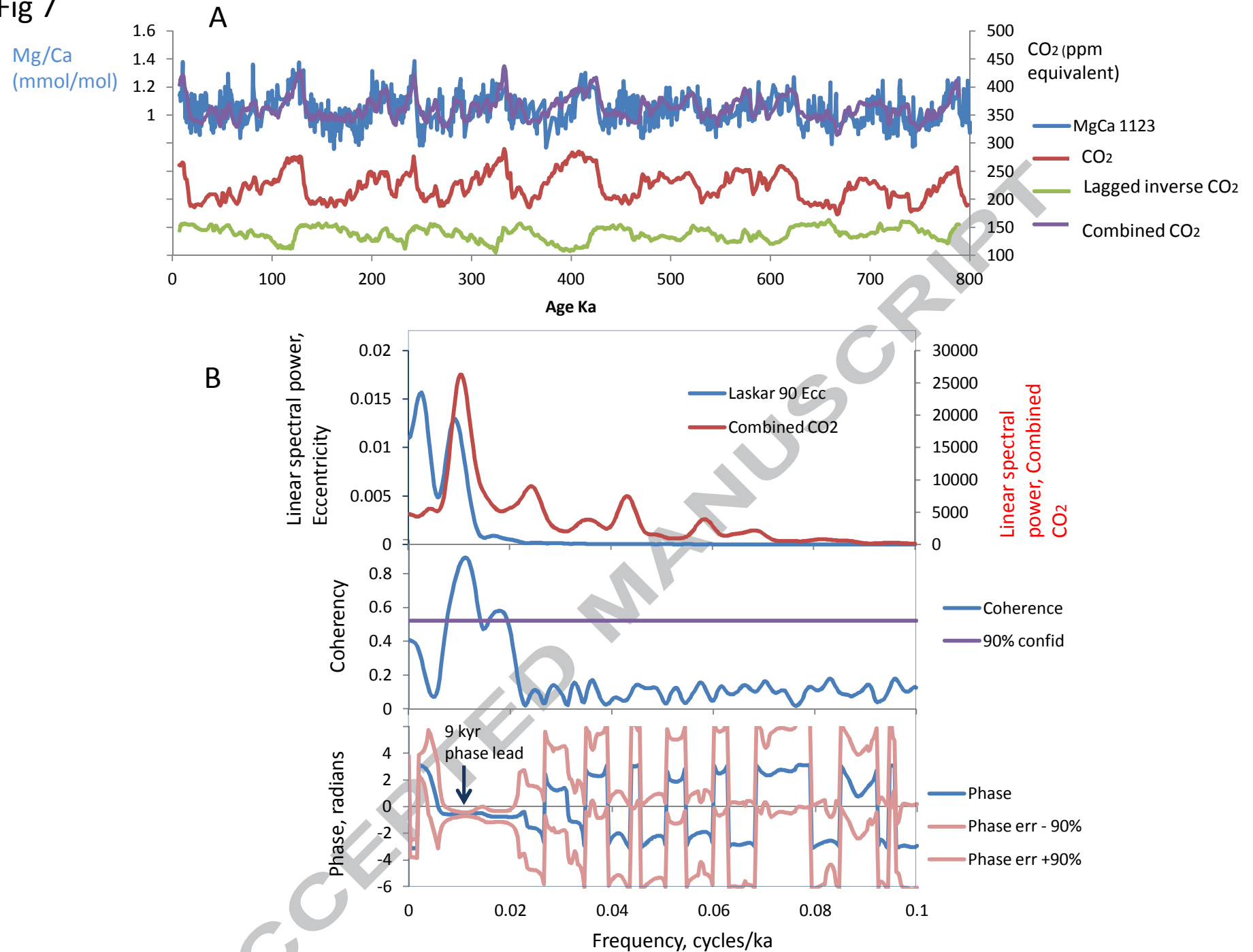


Fig 8

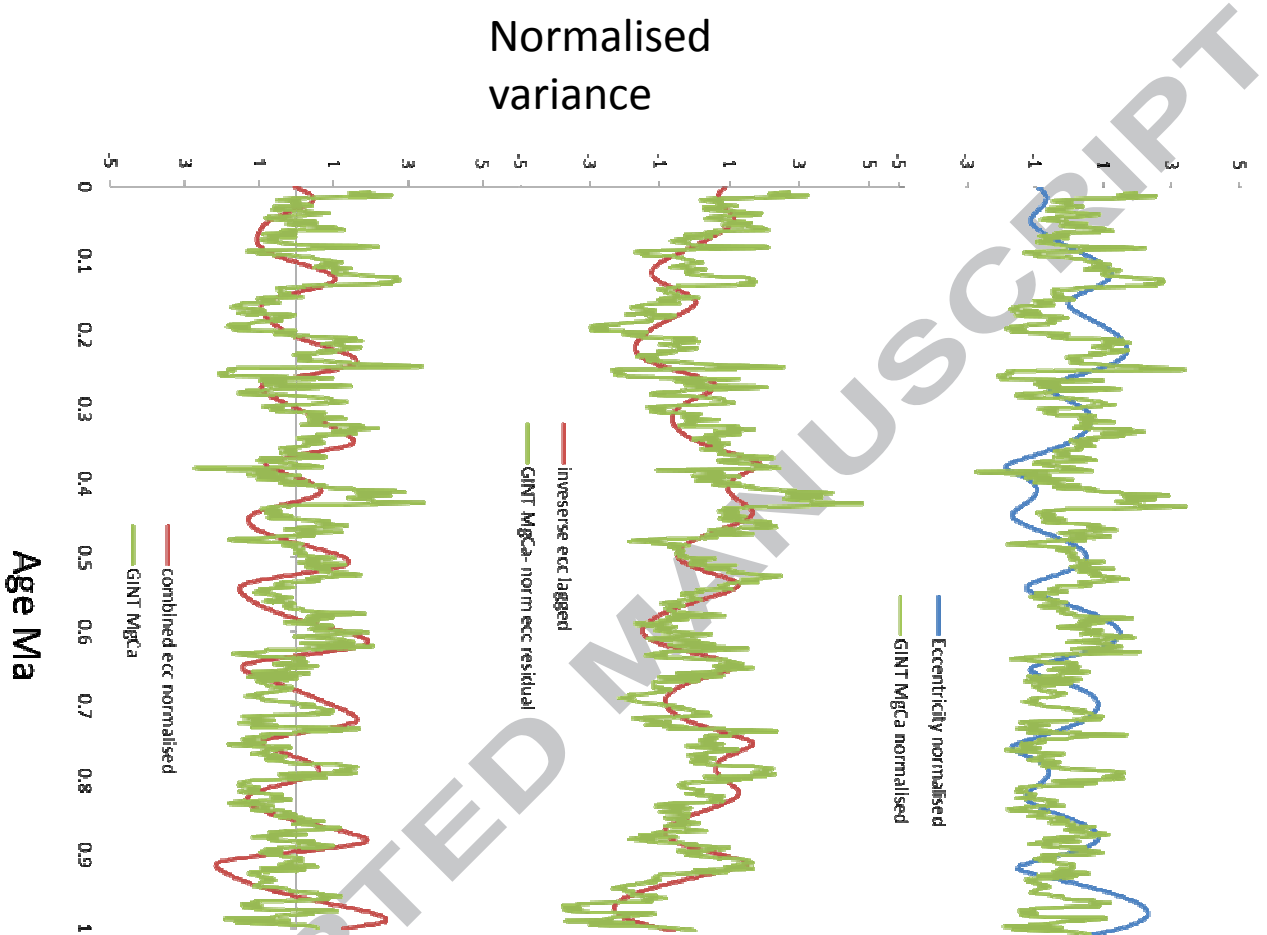


Fig 9

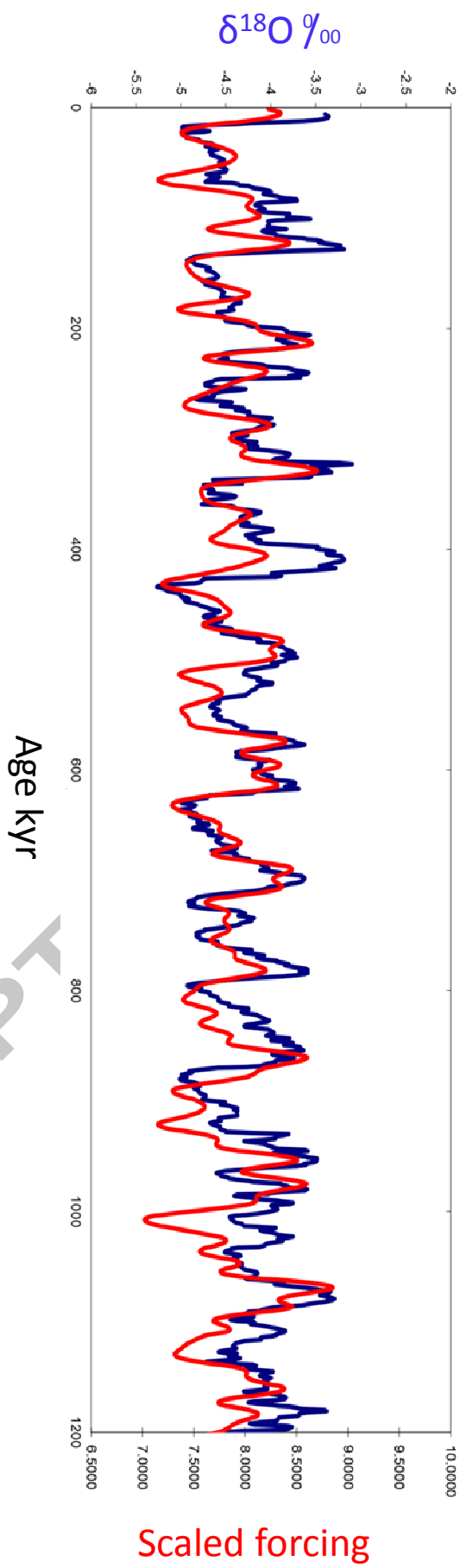


Fig 10

